River Flow 2020 – Uijttewaal et al (eds)

Morphodynamics of downstream fining in rivers with unimodal sand-gravel feed

C. An
Tsinghua University, Beijing, China

G. Parker
University of Illinois, Urbana-Champaign, USA

X. Fu
Tsinghua University, Beijing, China

M.P. Lamb
California Institute of Technology, Pasadena, USA

J.G. Venditti
Simon Fraser University, Vancouver, Canada

ABSTRACT: Rivers often show a downstream decrease in both the bed slope (long profile upward concavity) and bed surface characteristic grain size (downstream fining). Downstream fining is gradual, except at the gravel-sand transition, where bed grain size changes over short downstream distances, often only a few channel widths. A gravel-sand transition can be expected to arise when the sediment in transport is bimodal, with sand and gravel modes but a paucity of 1-10 mm gravel range. However, it has also been suggested that gravel-sand transitions may be generated autogenically, as decreasing bed slope in the downstream direction drives sand abruptly out of suspension and buries gravel which might be well under the threshold of motion. To study the problem of autogenic gravel-sand transitions, we propose a river morphodynamic model which erases any explicit distinction between gravel and sand transport. Such a distinction between gravel and sand is generally implemented in previous models of sediment transport and river morphodynamics. A unimodal mixture of sand and gravel is used in the present simulation to exclude the effect of bimodality of sediment on the gravel-sand transition. Upward concavity in the profile is forced through basin subsidence. We consider a river channel from a mountain valley to a subsiding foreland basin by implementing a spatially varying width of floodplain where sediment can deposit. Simulation results show that downstream fining is manifested throughout the entire reach, with an abrupt grain size transition occurring immediately downstream of where the floodplain width increases dramatically and gravel deposits as the river comes into the foreland basin.

1 INTRODUCTION

Rivers often show long-profile upward concavity and downstream fining in their bed material. Characteristic bed grain size may not fine monotonically, but instead have a distinct break in the gradual downstream fining profile called the gravel-sand transition (GST). The GST is characterized by an abrupt decrease in grain size, with bed materials changing from gravel to sand (Yatsu, 1955; Venditti and Church, 2014; Blom et al., 2017).

Several mechanisms have been proposed for the emergence of a GST. The first mechanism is related to the crystalline lithology of source rocks, where fine gravel disintegrates directly

into sand-size grains, leading to a grain size gap between 1 mm and 10 mm (Yatsu, 1955). The second mechanism relates the GST to external controls that lead to a rapid decline in transport capacity, such as a backwater effect generated by a set base level (Sambrook Smith and Ferguson, 1995), as well as distributary channels in river deltas (Dong et al., 2016). The third mechanism can be regarded as an autogenic process associated with the selective transport of sediment mixtures of sand and gravel in bedload (e.g., Ferguson, 2003). Based on data for the Fraser River, Canada, Venditti and Church (2014) describe a forth selective transport process driven by suspended load: as the slope declines, gravel movement ceases and sand comes out of suspension, which eventually buries the gravel bed and completes the gravel-sand transition. Lamb and Venditti (2016) developed a simple model to show the plausibility of this mechanisms by analyzing the threshold for sand transport in washload. Here we build on that work by implementing a one-dimensional morphodynamic model.

2 MORPHODYNAMIC MODEL

A one-dimensional morphodynamic model is implemented to study the problem of gravel-sand transitions. In the model, flow hydraulics are calculated with the normal flow assumption,

$$h = \left(\frac{{q_w}^2}{g S {C_z}^2}\right)^{1/3} \tag{1}$$

where h is the flow depth, q_w is the flow discharge per unit width, g = 9.81 m/s^2 is the gravitational acceleration, S is the longitudinal bed slope, C_z is the dimensionless Chézy coefficient, calculated in the model as (Parker, 2004).

$$C_z = 2.26 S^{-0.21} \tag{2}$$

Sediment conservation is described in the model by the Exner equation with an active layer formulation. Subsidence of the river basin is introduced in the model to generate an upward concave profile (i.e., reduction in longitudinal bed slope S in the streamwise direction).

$$(1-\lambda_p)\left(\frac{\partial \eta}{\partial t} + \sigma\right) = -\frac{I_f \Omega \Lambda}{r_B}\frac{\partial q_{tT}}{\partial x} \tag{3}$$

$$(1-\lambda_p)\left[L_a \frac{\partial F_i}{\partial t} + (F_i - f_{Ii})\frac{\partial L_a}{\partial t}\right] = \frac{I_f \Omega \Lambda}{r_B}\left(-\frac{\partial q_{ti}}{\partial x} + f_{Ii}\frac{\partial q_{tT}}{\partial x}\right) \tag{4}$$

where λ_p is the porosity of sediment deposit, taken as 0.3, η is bed elevation, σ is the subsidence rate, I_f is the flood intermittency factor, Ω is the channel sinuosity, Λ is the ratio of wash load deposited per unit bed material load deposited, r_B is the ratio of floodplain width to channel width, q_{tT} is the total sediment transport rate per unit width, q_{ti} is the sediment transport rate per unit width for the i-th size range, F_i is the fraction of the i-th size range on bed surface, f_{Ii} is the fraction of the i-th size range exchanged between the substrate and the active layer, and L_a is the thickness of the active layer, with

$$L_a = n_a h \tag{5}$$

$$f_{Ii} = \begin{cases} f_i|_{\eta - L_a} & \frac{\partial q_{tT}}{\partial x} > 0 \\ \alpha F_i + (1-\alpha) p_{ti} & \frac{\partial q_{tT}}{\partial x} \le 0 \end{cases} \tag{6}$$

where n_a is a nondimensional parameter specified as 0.1, $f_i|_{\eta\text{-}La}$ is the fraction of the i-th size range toward the top of substrate layer, p_{ti} is the fraction of the i-th size range in sediment load, and α is a nondimensional parameter specified as 0.5 (Hoey and Ferguson, 1994; Toro-Escobar et al., 1996).

The sediment transport rate in equations (3) and (4) is calculated as the sum of bedload and suspended bed material load in our model. The Ashida and Michiue (1972) relation is implemented for the calculation of the bedload transport rate. For the bed material suspended load (rather than wash load), most existing methods are developed for sand mixtures and do not have the ability to deal with sand-gravel mixtures. An et al. (in preparation) have modified the Wright and Parker (2004) entrainment relation to cover the range of gravel as well as sand. Here we implement the extended Wright-Parker (An et al., in preparation) formulation for the calculation of bed material suspended load.

3 NUMERICAL MODELING

3.1 *Computational conditions*

River morphodynamic modeling is conducted in a channel with a reach length of 40 km and a constant channel width of 500 m. Water and sediment supply are introduced from the upstream end, with a water supply rate per unit width of 3 m^2/s and the annual sediment supply rate of 4 Mt/a. A uniform subsidence rate of 5 mm/a is introduced in the whole channel reach in order to generate an upward concave profile. The ratio of floodplain width to channel width (r_B) is specified as 3 for the 8.8 km upstream reach and 60 for remaining 31.2 km downstream reach. This mimics a river channel exiting a mountain valley into a foreland basin, with a drastic increase in the floodplain width at the entrance to the foreland basin (cf. Dingle et al., in review). The simulation starts from an initial channel with a longitudinal slope of 0.002. The grain size distribution of the sediment supply and the initial bed material is presented in Figure 1. A unimodal grain size distribution is implemented in the simulation. This unimodality excludes the effect of bimodality of sediment on the gravel-sand transition. The sediment consists of 50% gravel and 50% sand. Other parameters implemented in the simulation are summarized in Table 1.

3.2 *Simulation results*

Figure 2 shows the temporal variations of both the longitudinal profile (bed elevation and longitudinal bed slope) and the bed surface texture (surface geometric mean grain size D_{sg} and

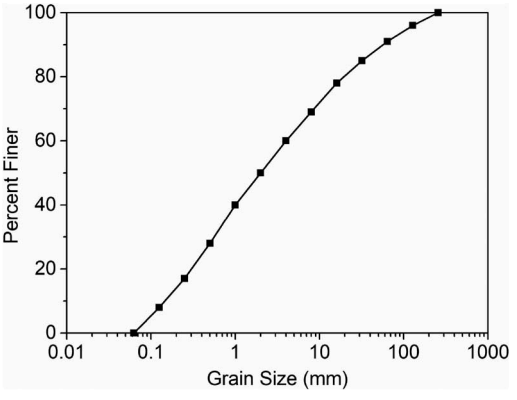

Figure 1. Grain size distribution of the sediment supply and the initial bed material (including active layer and substrate).

Table 1. Summary of computational conditions.

Parameter	Value
Channel length L	40 km
Channel width B	500 m
Initial slope S_I	0.002
Inflow discharge Q_{wf}	1500 m^3/s
Annual sediment supply G_{tf}	4 Mt/a
Flood intermittency factor I_f	0.025
Subsidence rate σ	5 mm/a
Ratio of floodplain width to channel width r_B	3 for the upper 8.8 km reach; 60 for the lower 31.2 km reach
Ratio of wash load deposited per unit bed material load deposited Λ	1
Channel sinuosity Ω	1.5
Cell size Δx	1.6 km
Time step Δt	1.25×10^{-3} year

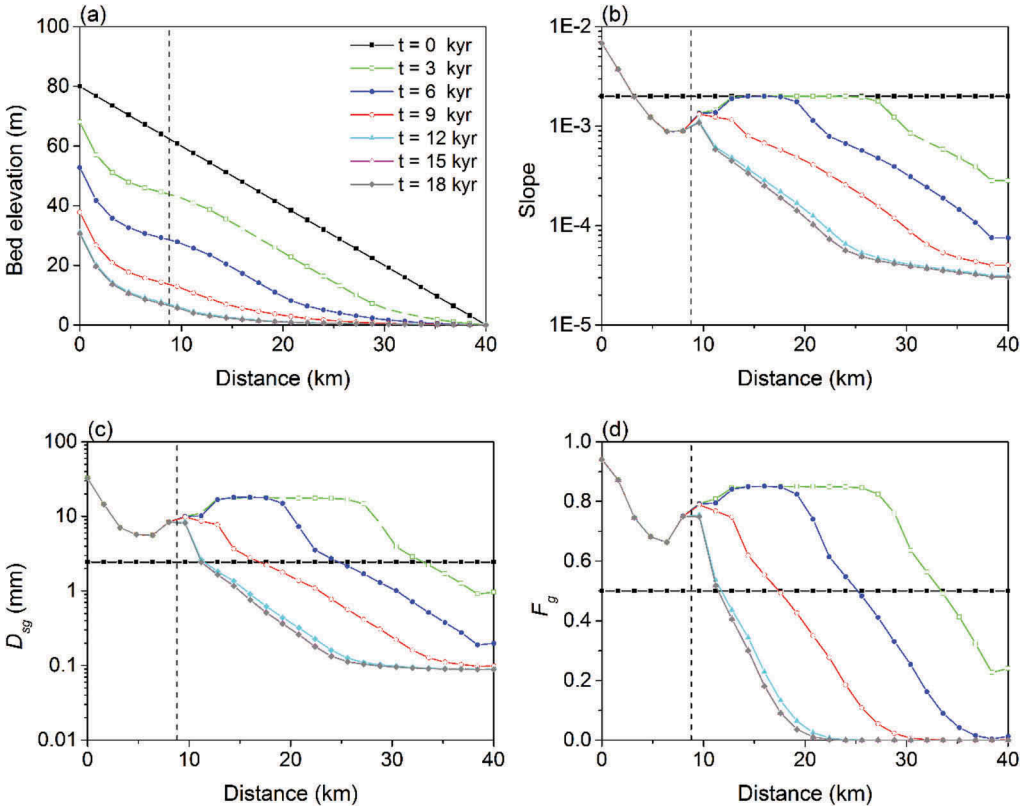

Figure 2. Simulation results of the transient process and equilibrium of the downstream fining morphodynamics. (a) Bed elevation, (b) longitudinal bed slope, (c) surface geometric mean grain size D_{sg}, (d) fraction of gravel on bed surface F_g. The vertical dashed line denotes x = 8.8 km where the drastic increase in the floodplain width occurs (nodes upstream of x = 8.8 km correspond to r_B = 3 and nodes downstream of x = 8.8 km correspond to r_B = 60).

fraction of gravel on bed surface F_g) of the river. The simulation duration is 18,000 years. The simulation shows that the river reached equilibrium at ~12,000 years, with only slight temporal adjustment afterwards (the lines for 12,000, 15,000 and 18,000 years plot nearly on top of each other).

Figure 2(a) shows that the river profile experiences degradation from the initial profile, under the specified water/sediment supply and subsidence rate. The river longitudinal profile exhibits upward concavity at steady state. Upward concavity of the steady-state profile is also shown in Figure 2(b) in terms of the downstream decrease in the channel slope. Moreover, the downstream decrease in the channel slope is not monotonic, but shows a slight increase in channel slope around x = 8.8 km, where the drastic increase in the floodplain width (r_B = 3 to r_B = 60) occurs. Figure 2(c) and Figure 2(d) show the downstream fining of the bed surface in terms of the geometric mean grain size D_{sg} and the fraction of gravel on bed surface F_g. Again, the downstream fining is not monotonic, but shows a slight increase of both D_{sg} and F_g around x = 8.8 km. The slight increase in the slope, D_{sg}, and F_g is related to the deposition of coarse sediment as a result of the drastic increase in the floodplain width (which can lead to a sudden decrease of sediment load). The drastic increase in the floodplain width induces a gravel-sand transition from a unimodal gravel-sand mixture, with the D_{sg} decreasing from 8.4 mm at x = 8 km to 0.8 mm at x = 16 km, and F_g decreasing from 0.75 at x = 8 km to 0.18 at x = 16 km. Such a gravel-sand transition can be ascribed to the different response of sediment in each size class (i.e., selective transport) to the drastic increase in the floodplain width.

4 CONCLUSIONS

In this paper, river morphodynamic modeling is implemented to investigate the autogenic gravel-sand transition. Explicit distinctions between gravel and sand transport, which are generally implemented in previous models of sediment transport and river morphodynamics, are erased in the model of this paper. A unimodal mixture of sand and gravel is used in the simulation to exclude the effect of bimodality of sediment on the autogenic gravel-sand transition. A river channel from a mountain valley to a subsiding foreland basin is considered by implementing a spatially varying width of flood plain where sediment can deposit. Simulation results show that upward concavity in the longitudinal profile and downstream fining in the bed material are manifested throughout the entire reach under the condition of basin subsidence. An abrupt grain size transition occurs immediately downstream of where the floodplain width increases dramatically and gravel deposits as the river comes into the foreland basin. Our simulation results support the mechanism of autogenic gravel-sand transition as proposed by Venditti and Church (2014).

ACKNOWLEDGEMENTS

The participation of An was supported by grant from China Postdoctoral Science Foundation (grant 2018M641368). The participation of Parker was supported in part by Tsinghua University through a visiting professorship, and in part by the W. H. Johnson Professorship, University of Illinois Urbana-Champaign, USA. The participation of Fu was supported by grants from the National Natural Science Foundation of China (grants 51525901 and 91747207).

REFERENCES

An, C., Parker, G., Fu, X., Lamb, M.P., & Venditti, J.G. in preparation. A unified river morphodynamic model for gravel sand transport and its application to the downstream fining in rivers with unimodal sand-gravel feed.

Ashida, K., & Michiue, M. 1972. Study on hydraulic resistance and bedload transport rate in alluvial streams. *Transactions Japan Society of Civil Engineering* 206: 59–69 (in Japanese).

Blom, A., Chavarrías, V., Ferguson, R.I., & Viparelli, E. 2017. Advance, retreat, and halt of abrupt gravel-sand transitions in alluvial rivers. *Geophysical Research Letters* 44: 9751–9760. https://doi.org/10.1002/2017GL074231.

Dingle, E.H., Sinclair, H.D., Venditti, J.G., Attal, M., Kinnaird, T.C., Creed, M., Quick, L., & Nittrouer, J. A. in review. Controls on channel migration and floodplain recycling across gravel-sand transitions. *Geology*.

Dong, T.Y., Nittrouer, J.A., Il'icheva, E., Pavlov, M., McElroy, B., Czapiga, M.J., Ma, H., & Parker, G. 2016. Controls on gravel termination in seven distributary channels of the Selenga River Delta, Baikal Rift basin, Russia. *GSA Bulletin* 128(7/8): 1297–1312. Doi: 10.1130/B31427.1.

Ferguson, R.I. 2003. Emergence of abrupt gravel to sand transitions along rivers through sorting processes. *Geology* 31(2): 159–162.

Hoey, T.B., & Ferguson, R. 1994. Numerical simulation of downstream fining by selective transport in gravel bed rivers: Model development and illustration. *Water Resources Research* 30(7): 2251–2260. Doi: 10.1029/94WR00556.

Lamb, M.P., & Venditti, J.G. 2016. The grain size gap and abrupt gravel-sand transitions in rivers due to suspension fallout. *Geophysical Research Letters* 43: 3777–3785. Doi: 10.1002/2016GL068713.

Parker, G. 2004. *1D sediment transport morphodynamics with applications to rivers and turbidity currents*, available at: http://hydrolab.illinois.edu/people/parkerg//morphodynamics_e-book.htm.

Sambrook Smith, G.H., & Ferguson, R. I. 1995. The gravel-sand transition along river channels. *Journal of Sedimentary Research* 65(2A): 423–430. https://doi.org/10.1306/D42680E0-2B26-11D7-8648000102C1865D.

Toro-Escobar, C.M., Parker, G., & Paola, C. 1996. Transfer function for the deposition of poorly sorted gravel in response to streambed aggradation. *Journal of Hydraulic Research* 34(1): 35–53. Doi: 10.1080/00221689609498763.

Venditti, J.G., & Church, M. 2014. Morphology and controls on the position of a gravel-sand transition: Fraser River, British Columbia. *Journal of Geophysical Research: Earth Surface* 119: 1959–1976. https://doi.org/10.1002/2014JF003147.

Wright, S., & Parker, G. 2004. Flow resistance and suspended load in sand-bed rivers: simplified stratification model. *Journal of Hydraulic Engineering* 130(8): 796–805.

Yatsu, E. 1955. On the longitudinal profile of the graded river. *Eos, Transactions American Geophysical Union* 36(4): 655–663. https://doi.org/10.1029/TR036i004p00655.